Posttraumatic Headaches and Postcraniotomy Syndromes

Allison Weyer, MD

KEYWORDS

• Posttraumatic • Postcraniotomy • Hemorrhage • Herniation • Fracture • Injury

KEY POINTS

- Headache is one of the most common sequelae of traumatic brain injury, and imaging is often warranted to evaluate for posttraumatic intracranial abnormalities that may present with headache.
- Many patients experience headache after craniotomy. Imaging identifies postoperative complications and guides management.
- CT and MRI of the brain contribute to the diagnostic evaluation of patients with headache following trauma or craniotomy.
- CT is usually the best initial imaging modality, whereas MRI is more sensitive for particular posttraumatic and postoperative abnormalities.

Abbreviations	
CTA	computed tomography angiography
SDH	subdural hematoma
FLAIR	fluid attenuated inversion recovery
MRI	magnetic resonance imaging
DWI	diffusion weighted imaging
ADC	apparent diffusion coefficient
ICA	internal carotid artery

INTRODUCTION

Disturbance or violation of the intracranial compartment by trauma or surgery may result in headache. The headaches associated with trauma and craniotomy range in severity from mild to severe. The time course of onset also varies from immediate to delayed. Some of the entities discussed have complex clinical presentations with multiple symptoms and signs, of which headache may be one. Several posttraumatic and postcraniotomy pathologies that may manifest with headache are discussed in the following sections with a focus on their imaging appearances.

Division of Neuroradiology, University of Pittsburgh Medical Center, 200 Lothrop Street, South Tower, 2nd Floor, Suite 200, East Wing, Pittsburgh, PA 15213, USA
E-mail address: weyerag2@upmc.edu

Neurol Clin 40 (2022) 609–629
https://doi.org/10.1016/j.ncl.2022.02.003 **neurologic.theclinics.com**

DISCUSSION

POSTTRAUMATIC HEADACHES

Posttraumatic headache is described in the International Classification of Headache Disorders (ICHD) as a secondary headache that begins within 7 days following trauma or within 7 days after recovering consciousness or the ability to sense and report pain.[1] It is one of the most common sequelae of traumatic brain injury: the 1-year cumulative incidence of new or worsened headache in patients with mild traumatic brain injury (mTBI) has been reported as 91%.[2] Several intracranial traumatic abnormalities are associated with headache, and their imaging features are discussed in detail below.

American College of Radiology Appropriateness Criteria

The American College of Radiology (ACR) publishes Appropriateness Criteria, which are evidence-based guidelines for selecting appropriate diagnostic imaging for various clinical conditions. The Appropriateness Criteria for imaging head trauma are referenced in the following text and provide recommendations for which imaging examination to order in specific contexts. Although specific points are discussed subsequently, it is important to note that noncontrast head CT is usually appropriate for the initial imaging of acute head trauma that is moderate or severe (Glasgow Coma Scale [GCS] 3–12) or penetrating.[3] Noncontrast head CT is also usually appropriate for the initial imaging of mild acute head trauma (GCS 13–15) when imaging is indicated by a clinical decision rule.[3] This is due to the speed and accessibility of CT imaging as well as to the sensitivity of this modality for detecting hemorrhage, herniation, and infarction that may warrant neurosurgical intervention.[4]

Reviewing thin-section reconstructions of a noncontrast head CT in the coronal and sagittal planes improves the detection of intracranial hemorrhage and is recommended when evaluating a patient presenting with acute head trauma.[5,6]

Subdural Hematoma

Subdural hematomas are collections of blood products between the dura and the arachnoid mater that usually result from tears in bridging cortical veins. They do not cross midline but instead track along the falx under the dura. Unlike epidural hematomas, they are not confined by the dural attachments associated with calvarial sutures, and their classic morphology is therefore crescentic (**Fig. 1**).

Acute subdural hematomas are usually hyperdense relative to brain parenchyma on CT and become less dense as the blood products age. Although there are no precise time intervals when blood products demonstrate specific densities, a systematic literature review described mixed and hyperdense subdural hematomas reported after a median time interval of 1 and 2 days, respectively, whereas isodense and hypodense subdural hematomas were reported after 11 and 14 days, respectively.[7] The presence of blood products of different densities within a subdural hematoma is often attributed to acute-on-chronic hemorrhage. However, isodensity or hypodensity does not always indicate older blood. Nonclotted blood will seem hypodense, and this may be observed in the setting of hyperacute hemorrhage (see **Fig. 1**; **Fig. 2**) or chronic hemorrhage in a patient with coagulopathy. Blood may seem isodense to brain parenchyma if it is subacute, but this appearance can also occur if the patient is anemic or if there is mixing of CSF with acute blood in the setting of an arachnoid tear.

Although MRI is not recommended in the initial imaging of acute head trauma, it may be indicated to evaluate persistent neurologic deficits that are not explained by the initial head CT. Small subdural hematomas are more sensitively detected with MRI than with CT. MRI may also play a role in planning surgical evacuation of subdural

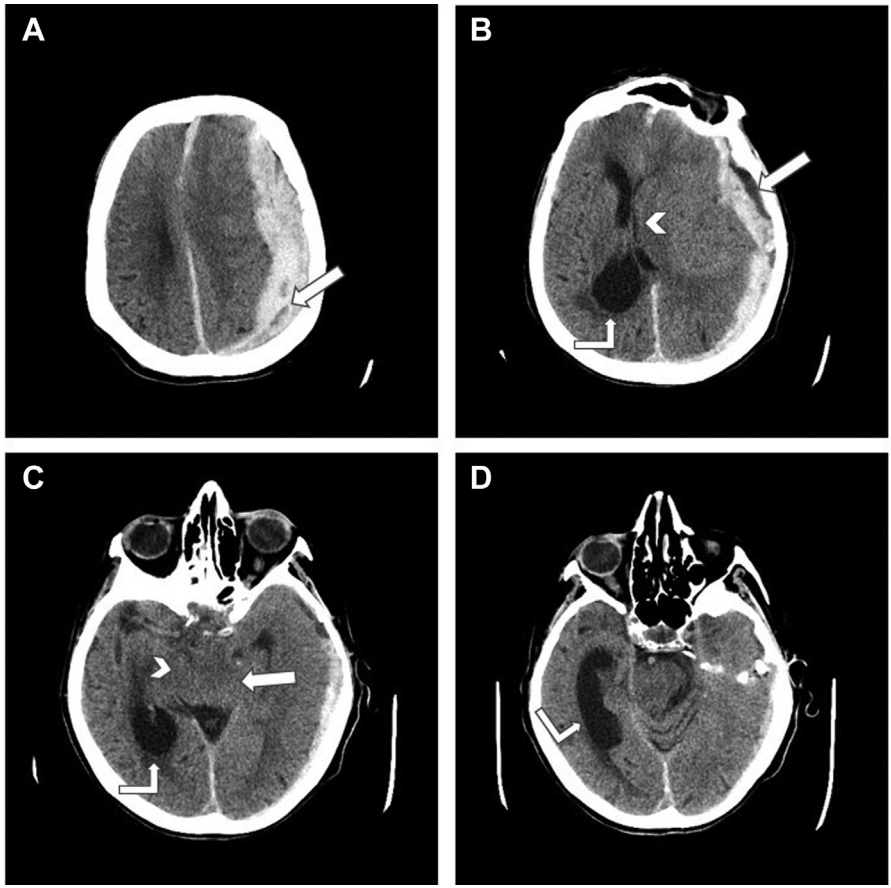

Fig. 1. Hyperacute subdural hematoma in an elderly woman who was found down and last seen well 3 hours prior. (*A*) Axial noncontrast head CT image shows a large crescentic left cerebral convexity SDH that contains low-density hyperacute nonclotted blood products mixed with hyperdense hemorrhage. This is known as the swirl sign (*arrow*). (*B*) Axial noncontrast head CT image at the level of the foramen of Monro again shows hyperacute, mixed-density left SDH (*straight arrow*) with rightward subfalcine herniation (*arrowhead*) and asymmetric dilation of the right lateral ventricle (*angled arrow*) indicating ventricular entrapment. (*C*) Axial noncontrast head CT image at the level of the midbrain demonstrates left uncal herniation (*straight arrow*) as well as partial effacement of the right ambient cistern (*arrowhead*). Entrapment of the right lateral ventricle is also visualized at this level (*angled arrow*). (*D*) Axial noncontrast head CT image demonstrates marked dilation of the temporal and occipital horns of the right lateral ventricle compatible with entrapment (angled *arrow*).

hematomas with subacute or chronic components by demonstrating the presence and location of septations within the hematoma[8,9] (**Fig. 3**). The risk of recurrence of a subdural hematoma following evacuation may also be predicted based on the appearance of blood on T1-weighted and T2-weighted sequences.[10]

Subdural Hygroma

Posttraumatic subdural hygromas are collections of CSF in the subdural compartment, which result from tears of the arachnoid. Because they follow the same density and

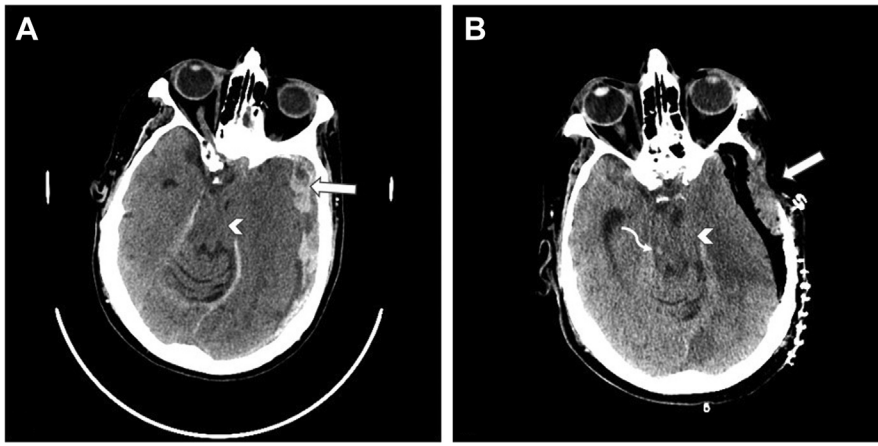

Fig. 2. Hyperacute subdural hematoma with uncal herniation and Duret hemorrhage. (*A*) Axial noncontrast CT image of the head shows the swirl sign of a hyperacute left subdural hematoma (*arrow*) as well as uncal herniation (*arrowhead*). (*B*) Axial noncontrast CT image of the head shows interval left craniectomy for evacuation of the subdural hematoma (*arrow*) with persistent uncal herniation (*arrowhead*) and new punctate hyperdensity in the right dorsal midbrain (curved *arrow*) compatible with acute parenchymal hemorrhage that is known as Duret hemorrhage in the setting of severe uncal herniation.

signal characteristics on CT and MRI as does normal CSF, they may be difficult to distinguish from the normal CSF surrounding the brain, especially in the setting of brain atrophy. However, hygromas will displace the cortical veins away from the calvarium and are often observed in combination with other posttraumatic findings in the brain.

Hygromas tend to appear later following trauma than acute hematomas, with a mean time to appearance of 9 days after injury.[11] However, they may also occur in the first day after injury. Although they should follow the appearance of CSF on all

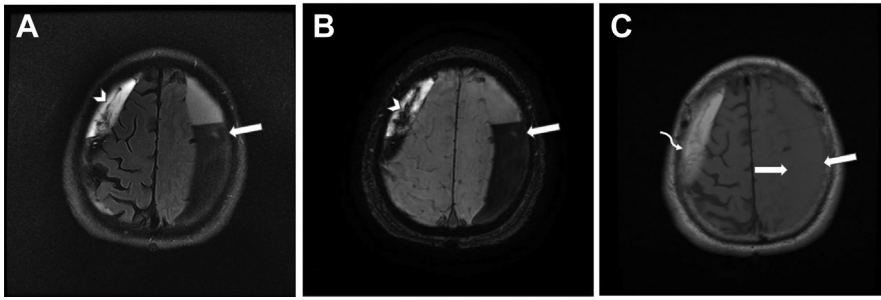

Fig. 3. Bilateral subdural hematomas of different ages. (*A*) Axial T2/FLAIR MR image of the brain shows T2 hypointense blood layering dependently within a chronic left subdural hematoma (*straight arrow*). Linear T2 hypointense structures within a chronic right subdural hematoma (*arrowhead*) represent septations. (*B*) Axial susceptibility-weighted MR image of the brain shows hypointensity associated with the dependent blood products (*straight arrow*) as well as with the septations in the right subdural hematoma (*arrowhead*). (*C*) Axial T1-weighted MR image of the brain shows isointense signal of the more recent left subdural hematoma (*arrow*) and hyperintensity of the subacute blood within the right subdural hematoma (*curved arrow*).

imaging, they may demonstrate transient hyperdensity if the patient recently received intravenous contrast. Dual-energy CT technique can be used to image the brain of a trauma patient who recently received contrast to distinguish between contrast and acute hemorrhage as the cause of hyperdensity within a subdural collection.[12]

Epidural Hematoma

Epidural hematomas are collections of blood products between the inner table of the calvarium and the dura. They are confined by the calvarial sutures because the dura is attached to the calvarium in these locations, and as a result, they tend to have a lenticular or biconvex shape. An epidural hematoma may only cross a suture if a fracture involves the suture.

Epidural hematomas can result from arterial or venous bleeding, but typically they are associated with injury to the middle meningeal artery in the setting of a calvarial fracture (**Figs. 4 and 5**). The presence of an epidural hematoma should prompt a search for a calvarial fracture and vice versa, although they can certainly occur in isolation of each other. Injury to a dural venous sinus may result in a venous epidural hematoma.

As discussed in the section on subdural hematomas, acute blood within an epidural hematoma is hyperdense on CT. However, hyperacute, unclotted blood may seem hypodense and mix with hyperdense hemorrhage, generating a "swirl sign" within an epidural hematoma[13] (shown within subdural hematomas in **Figs. 1 and 2**). This appearance of mixed densities within a hematoma should prompt urgent neurosurgical consultation, as it implies ongoing bleeding and potential rapid expansion of the hematoma. Although MRI is more sensitive for detecting subtle hemorrhage and for determining the age of blood products, it is reserved for evaluation of subacute or chronic head trauma with unexplained neurologic deficits or for follow-up if initial imaging was unremarkable but the patient has a persistent neurologic deficit.[3]

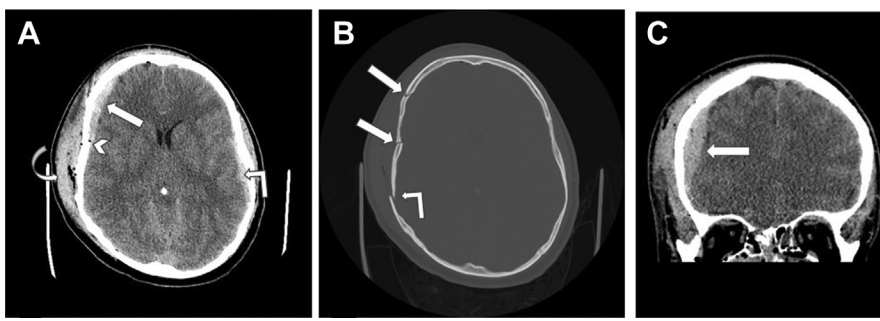

Fig. 4. Acute epidural hematoma in a middle-aged man who was the unhelmeted driver of a motorcycle that collided head-on with a car. (*A*) Axial noncontrast head CT image shows a crescentic acute extra-axial hematoma along the right frontal convexity (*straight arrow*) with a small amount of pneumocephalus (*arrowhead*) as well as soft tissue hemorrhage and gas in the overlying right scalp (*curved arrow*). There is also a contralateral extra-axial hematoma (*angled arrow*). On this image alone, it is difficult to determine whether the hematomas are epidural or subdural. (*B*) Axial noncontrast head CT in bone algorithm reveals multiple acute right calvarial fractures (*straight arrows*) with displacement posteriorly (*angled arrow*). (*C*) Coronal noncontrast head CT shows the classic lentiform, biconvex configuration of the acute EDH along the right frontal convexity (*arrow*).

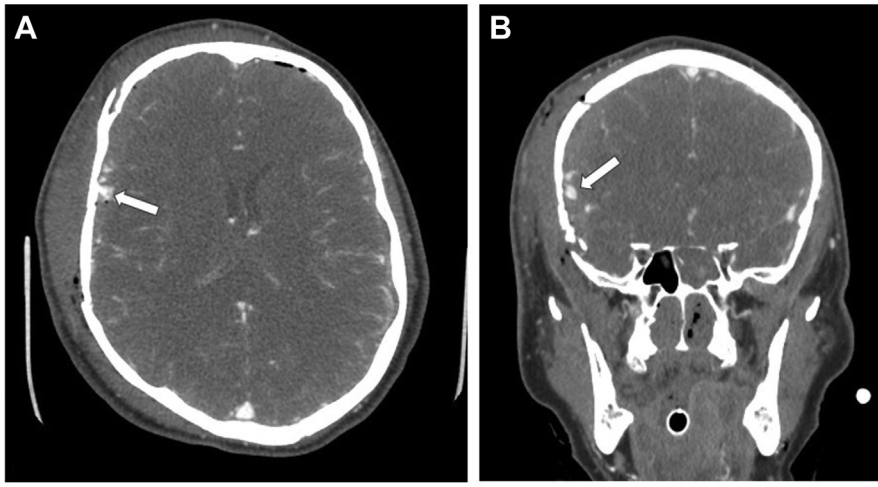

Fig. 5. Active bleeding into the epidural hematoma in the patient shown in Fig. 4. Axial (*A*) and coronal (*B*) CT angiographic images of the head show arterial phase contrast extravasation (*arrows*) into the epidural hematoma.

Subarachnoid Hemorrhage

Subarachnoid hemorrhage is located between the arachnoid and pia mater and insinuates within the sulci of the brain. It is generally of smaller volume than subarachnoid hemorrhage caused by aneurysm rupture and tends to be located at or opposite the site of impact (Fig. 6). It may also be observed in the basal cisterns, although isolated, cisternal subarachnoid hemorrhage is more often related to ruptured aneurysm and should prompt evaluation for aneurysm. Traumatic subarachnoid hemorrhage may redistribute into the ventricular system, where it may layer dependently or adhere to the ependyma or to the choroid plexus within the ventricles. Intraventricular

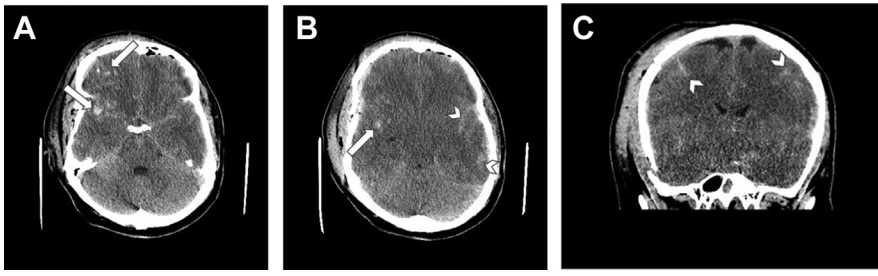

Fig. 6. Brain contusions and subarachnoid hemorrhage in the patient shown in Fig. 4 and 5. (*A*) Axial noncontrast head CT image shows multiple small acute parenchymal hemorrhages in the right frontal and anterior temporal lobes (*arrows*) compatible with traumatic contusions. (*B*) Axial noncontrast head CT image at a level superior to that in image *A* shows additional right brain contusion (*arrow*) as well as acute subarachnoid hemorrhage in several left cerebral sulci (*arrowheads*). (*C*) Coronal noncontrast head CT image shows acute subarachnoid hemorrhage in several bilateral cerebral sulci (*arrowheads*). Traumatic subarachnoid hemorrhage tends to be of lower volume than that caused by ruptured aneurysm.

hemorrhage can also arise from a ruptured subependymal vein or via extension from a parenchymal hematoma.

Certain locations of traumatic subarachnoid hemorrhage in the brain are associated with other traumatic brain abnormalities. Hemorrhage in the ambient cisterns or interhemispheric fissure on initial head CT has been shown to be a marker of severe diffuse axonal injury (DAI).[14] DAI has also been correlated with intraventricular hemorrhage on initial head CT.[15] Vasospasm is less commonly observed with traumatic subarachnoid hemorrhage than with aneurysmal hemorrhage, although a significant risk for vasospasm has been reported in the setting of severe traumatic brain injury.[16] MRI is more sensitive than CT in detecting small volumes of subarachnoid hemorrhage, and MRI performed for short-term follow-up of a patient with persistent neurologic deficit and unremarkable initial head CT may reveal subtle subarachnoid hemorrhage that could not be visualized on CT.

Brain Contusion

Brain contusions are parenchymal "bruises" related to traumatic impact and most often are located in the inferior-anterior frontal and temporal lobes, at coup-contrecoup sites (see **Fig. 6**). Initially, brain contusions may manifest on CT as hypodense areas of parenchymal edema with minimal or absent hyperdensity. During the 48 hours following injury, contusions often increase in size and develop progressively hyperdense areas of acute parenchymal hemorrhage. This phenomenon is described as "blossoming" or "blooming" of the contusion.[17] The hyperdense hemorrhage component often then resolves before the edema associated with the contusion. Serial imaging is therefore recommended for patients with brain contusions to monitor for progressive mass effect related to the edema, hemorrhage, or both.

The presence of a contusion has also been shown to contribute to the predicted clinical outcome of a patient. Temporal lobe contusions in particular were shown to be associated with a worse functional outcome 6 months following trauma than frontal contusions and extra-axial injuries.[18]

Depending on the age of the contusion, variable degrees of T1 and T2 signal and susceptibility artifact may be present on MRI. MRI is more sensitive than CT for detection of brain contusions, particularly when they are small, located near the calvarium or skull base, or lack hyperdense hemorrhage on CT.[19,20] This contributes to the ACR's determination that noncontrast MRI may be appropriate for short-term follow-up of patients with acute head trauma who have persistent neurologic deficits and normal head CTs.[3] The detection of subtle contusions in these patients, especially those with mild TBI, can assist with determining prognosis.[21]

Fracture

Calvarial and skull base fractures may occur as a result of blunt or penetrating trauma and are frequently associated with intracranial injuries such as epidural hematoma (as discussed above) and brain contusion. Acute fractures are best detected on noncontrast CT, and some fracture locations are associated with specific additional abnormalities. Fractures traversing the anterior cranial fossa are often associated with CSF leak,[22] and these patients may report headache features characteristic of intracranial hypotension. Imaging findings suggestive of CSF leak may include extra-axial CSF collection or pseudomeningocele, fluid collection in a paranasal sinus, and features of intracranial hypotension such as slumping midbrain and collapsed ventricles (**Fig. 7**). Noncontrast head, face, or temporal bone CT is usually adequate to identify the site of a CSF leak in the setting of head trauma, but if these studies

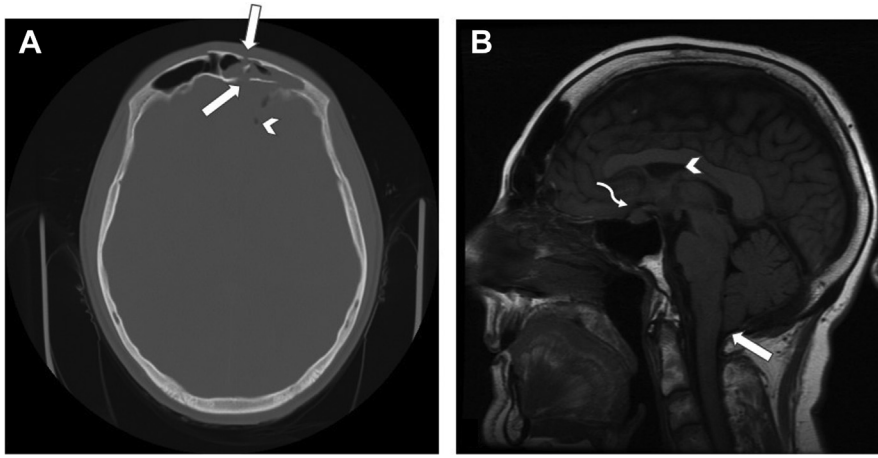

Fig. 7. Acute fractures traversing the left frontal sinus with subsequent intracranial hypotension presumed to relate to CSF leak. (*A*) Axial noncontrast CT image of the head in bone algorithm shows acute displaced fractures disrupting the outer and inner tables of the calvarium at the level of the left frontal sinus (*straight arrows*). A small amount of pneumocephalus is present (*arrowhead*). (*B*) Sagittal T1-weighted MR image of the brain 1 week later shows descent of the cerebellar tonsils into the foramen magnum (*arrow*), collapsed lateral ventricles (*arrowhead*), and effacement of the suprasellar cistern (*curved arrow*), all indicative intracranial hypotension. In the setting of recent fracture involving a paranasal sinus, the cause of the hypotension is most likely a CSF leak.

reveal multiple potential sites of leak, CT cisternography can be used to localize the precise site of CSF leak in order to guide surgical repair.[3,23]

Fractures involving a dural venous sinus or the jugular bulb can cause traumatic venous injury that leads to thrombosis or compression by an extra-axial hematoma.[24] Although findings suggestive of venous sinus injury may be present on noncontrast head CT, such as hyperdensity within a sinus or venous infarct, CT venography is the most useful imaging study to evaluate for suspected acute venous injury[3] (**Fig. 8**).

Long bone or pelvic fractures may rarely result in cerebral fat embolism, in which fat microemboli to the brain cause infarcts and petechial hemorrhage. This entity is best detected with MRI, where it may present with a range of imaging features such as scattered foci of restricted diffusion, areas of confluent T2 hyperintensity, and/or scattered foci of susceptibility artifact primarily in the white matter[25] (**Fig. 9**). The large number of foci of DWI hyperintensity scattered diffusely in the white matter has been described as the "starfield" pattern.[26] Although these patients may experience headache, more severe manifestations of cerebral fat embolism include delirium, seizures, and coma.[27]

Diffuse Axonal Injury

Shearing forces to the white matter can cause DAI. Acceleration–deceleration trauma that may be rotational or translational is associated with DAI and affects both the larger white matter tracts as well as the gray–white matter junction due to the sharp transition between tissues of different densities in this location.[4] MRI is the most sensitive imaging modality to detect DAI and may demonstrate hemorrhagic or nonhemorrhagic white matter lesions (**Fig. 10**). The location of the lesions indicates the severity of the injury per the following grading system: Grade 1 involves the subcortical white matter (at

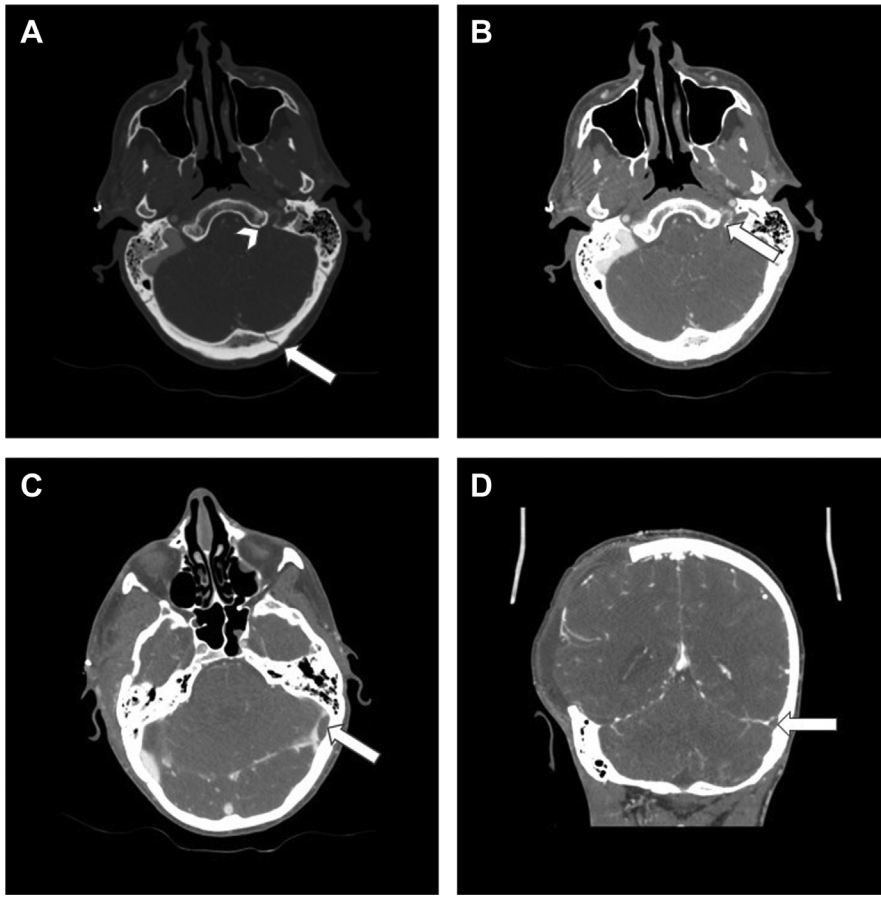

Fig. 8. Acute occipital calvarial fracture with associated sigmoid and transverse sinus thrombosis. (*A*) Axial CTA image of the head in bone algorithm shows acute nondisplaced fractures of the left occipital calvarium (*arrow*) and left aspect of the clivus (*arrowhead*). (*B*) Axial CTA image of the head shows a subocclusive filling defect of the left sigmoid sinus (*arrow*) compatible with thrombus. (*C*, *D*) Axial (*C*) and coronal (*D*) CTA images of the head show filling defect of the left transverse sinus (*arrows*) with both occlusive (*D*) and subocclusive (*C*) components.

the gray–white matter junction), Grade 2 involves the corpus callosum, and Grade 3 involves the brainstem.[28] DAI lesions restrict diffusion and may demonstrate susceptibility artifact. There may be associated or isolated T2 hyperintense lesions, although these are nonspecific and difficult to attribute to DAI in the absence of signal abnormalities on other sequences. Although both DAI and cerebral fat embolism may demonstrate multifocal susceptibility artifact and restricted diffusion in the white matter, the lesions of cerebral fat embolism tend to be more numerous and diffuse.

Diffusion tensor imaging (DTI) is an advanced imaging technique that has been applied to study patients with mTBI and posttraumatic migraines. Compared with mTBI patients without posttraumatic migraines, migrainous patients had DTI findings suggestive of injury to the corpus callosum and fornix.[29] This imaging tool is not yet used in routine clinical practice, but it has revealed patterns of injury that correlate with posttraumatic headaches.

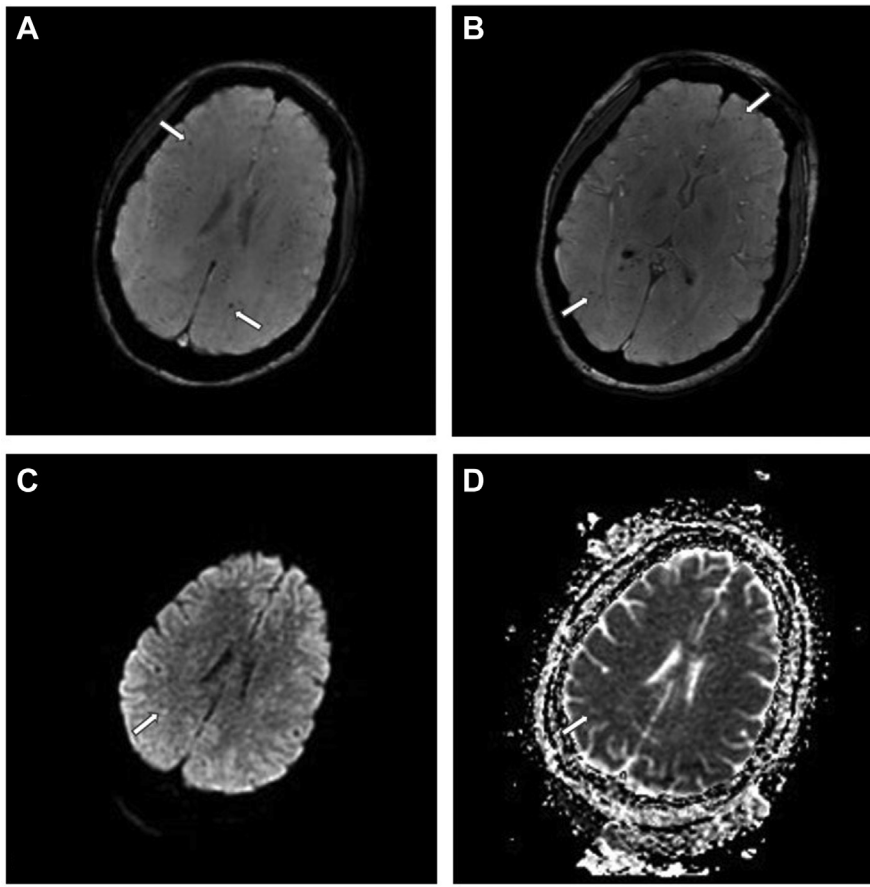

Fig. 9. Cerebral fat embolism in a 26-year-old patient with obtundation several days after sustaining pelvic fractures in a motor vehicle accident. (*A*, *B*) Axial susceptibility-weighted MR images of the brain show innumerable foci of hypointensity scattered diffusely throughout the white matter (*arrows*) most compatible with petechial hemorrhages related to fat microemboli to the brain. (*C*, *D*) Axial diffusion-weighted (*C*) and apparent diffusion coefficient (*D*) MR images of the brain show tiny foci of DWI hyperintensity and ADC hypointensity (*arrows*) compatible with restricted diffusion associated with the foci of susceptibility hypointensity. These are compatible with areas of ischemia and have been described as the "starfield" pattern.

Herniation

Mass effect associated with traumatic hemorrhage or edema in the brain may result in herniation, which can then cause secondary infarcts, hemorrhage, or hydrocephalus. Uncal or downward transtentorial herniation (see **Figs. 1 and 2**) may result in ipsilateral third nerve palsy and dilated pupil. The herniating brain can impress on the ipsilateral posterior cerebral artery and result in infarct in that territory. Bilateral or severe unilateral downward transtentorial herniation can also cause hemorrhage in the midbrain, referred to as Duret hemorrhage (see **Fig. 2**). The herniating brain in this setting may compress perforating arteries from the circle of Willis and result in basal ganglia or hypothalamic infarcts.

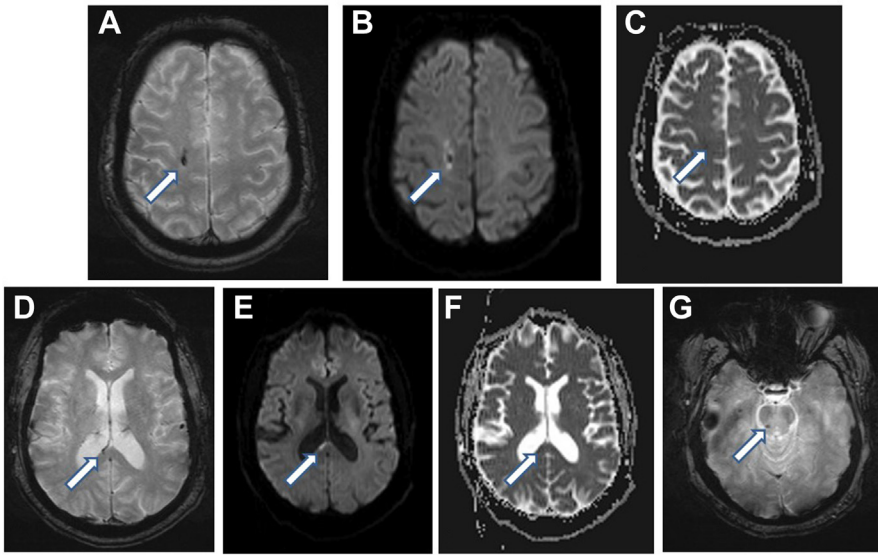

Fig. 10. DAI in a middle-aged man who was the unrestrained passenger in a motor vehicle collision. (*A*) Axial susceptibility-weighted MR image of the brain shows a hypointense focus in the right frontal white matter near the gray–white junction (*arrow*). There is corresponding hyperintensity that surrounds central hypointensity on diffusion-weighted image (*B*) and hypointensity on apparent diffusion coefficient image (*C*) compatible with restricted diffusion (*arrows*). This finding in isolation would indicate grade 1 DAI. (*D*) Axial susceptibility-weighted MR image of the brain in the same patient shows a hypointense focus in the splenium of the corpus callosum with corresponding restricted diffusion (*arrows*) (*E*, *F*). Involvement of the corpus callosum indicates grade 2 DAI. (*G*) Axial susceptibility-weighted MR image of the brain shows a hypointense focus in the dorsal midbrain (*arrow*) which indicates grade 3 DAI.

Subfalcine herniation can cause ipsilateral anterior cerebral artery territory infarction. If the herniating brain obstructs the foramen of Monro, the contralateral lateral ventricle can become dilated: this is referred to as ventricular entrapment (see Fig. 1). Cerebellar tonsillar herniation may obstruct the fourth ventricular outlet and cause hydrocephalus. If severe, this type of herniation can impress on the posterior inferior cerebellar artery and result in infarct in that territory. Ascending transtentorial herniation can obstruct the cerebral aqueduct and cause hydrocephalus at that level. The superior cerebellar arteries may be compressed in this setting and cause infarction.

Arterial Injury

Traumatic injury to the middle meningeal artery is discussed above in the section on epidural hematoma (see Fig. 5), but there are other arterial injuries that may result in headache. Traumatic injury to the cervical carotid artery more often presents with ipsilateral neck pain, neck hematoma, and possibly signs of infarct or cranial nerve palsy, although a traumatic aneurysm of this artery may result in headache.[30] Traumatic injury of the intracranial internal carotid artery may present with unilateral headache, as can injury to the intradural vertebral artery. CT angiography of the head and neck is usually appropriate to evaluate for arterial injury in patients with head trauma and

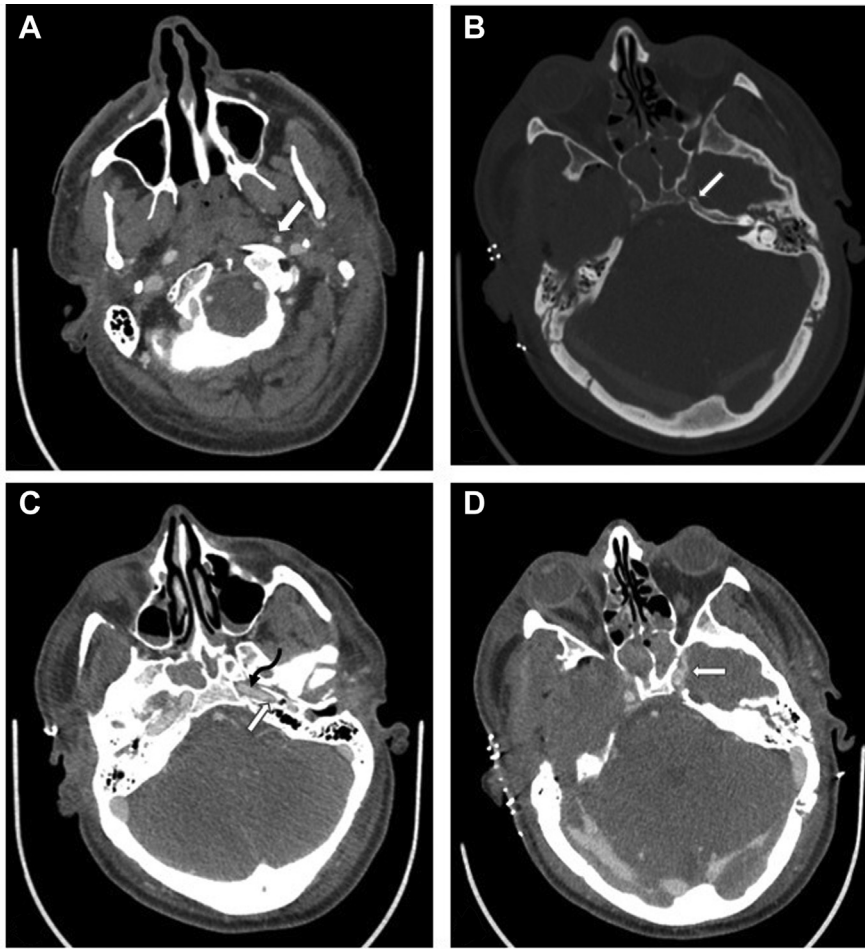

Fig. 11. Traumatic injury to the left cervical and intracranial ICA. (*A*) Axial CTA image of the head shows asymmetric smaller caliber of distal cervical left internal carotid artery relative to the right and slight irregularity (*arrow*) concerning for traumatic injury. (*B*) Axial CTA image of the head in bone algorithm shows an acute nondisplaced fracture involving the left carotid canal (*arrow*). (*C*) Axial CTA image of the head shows eccentric (*arrow*) and equivocal central linear (*black curved arrow*) filling defects in the petrous left ICA concerning for dissection and possible intimal flap. (*D*) Axial CTA image of the head shows asymmetric arterial phase contrast filling of the left cavernous sinus (*arrow*) concerning for traumatic carotid-cavernous fistula.

either clinical risk factors for vascular injury or imaging findings that may indicate vascular injury.[3] Imaging findings may include irregularity and narrowing of the injured artery and/or a linear filling defect compatible with intimal flap (**Fig. 11**). The presence of intracranial hemorrhage or infarct following trauma may prompt CTA, but skull base and cervical spine fractures are particularly concerning and warrant vascular imaging.

Traumatic carotid-cavernous fistula is a specific vascular injury that is associated with skull base fractures, particularly those involving the carotid canal. Damage to the intracranial internal carotid artery can lead to an arteriovenous shunt between

the artery and the adjacent cavernous sinus. Symptoms of this fistula include headache, orbital edema, and reduced vision and may present days following the injury or may be delayed and manifest several months later.[31] Noncontrast head CT and CTA may have findings suggestive of this fistula, such as dilation of the ipsilateral superior ophthalmic vein and cavernous sinus or arterial phase contrast filling of these venous structures (see **Fig. 11**). However, digital subtraction angiography is the definitive imaging tool when a traumatic carotid-cavernous fistula is suspected.

POSTCRANIOTOMY SYNDROMES

Although the ICHD classifies headache attributed to craniotomy as a type of posttraumatic headache,[1] some of the mechanisms and imaging features of postcraniotomy headaches are unique from those associated with noniatrogenic trauma. The ICHD describes a headache attributed to craniotomy as one that develops within 7 days after the craniotomy or within 7 days of regaining consciousness or discontinuing medications that impair the ability to sense or report headache.[1] To be attributed to craniotomy, a headache should not be better accounted for by another diagnosis. Postcraniotomy headache is common, with reported incidence of 60% when using the above definition.[32] There is a higher prevalence of headache when the duration of surgery is greater than 4 hours and when a craniectomy is performed rather than craniotomy or cranioplasty.[33] Some of the structural abnormalities and complications of craniotomy and their imaging appearances are discussed below.

Hemorrhage, Edema, and Pneumocephalus

A small amount of extra-axial hemorrhage is expected deep to a craniotomy immediately postoperatively, but if the hematoma is larger than generally observed, increases during serial imaging examinations, and/or causes mass effect (**Fig. 12**), it may

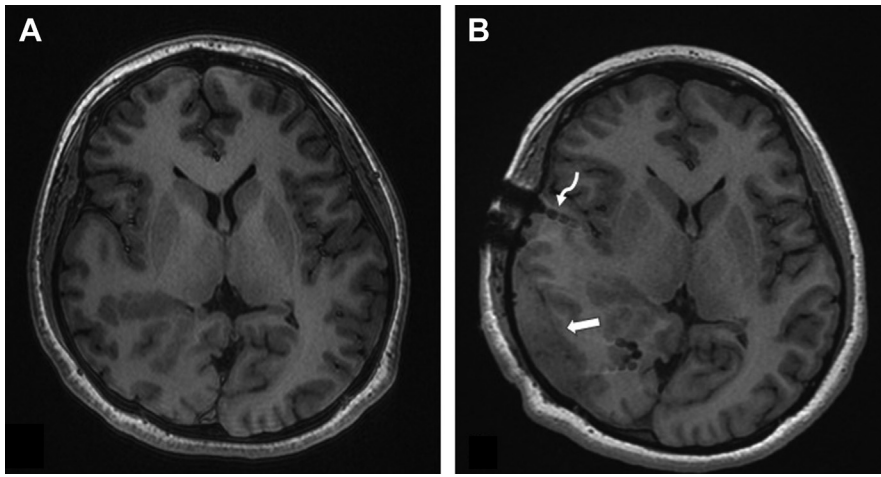

Fig. 12. Large subdural hematoma following placement of stereotactic EEG electrodes. Axial 3D T1-weighted MR images of the brain before (*A*) and following (*B*) placement of intracranial stereotactic EEG electrodes (*curved arrow*) shows a right parietotemporal subdural collection that is isointense to brain and new from the preoperative examination compatible with subdural hematoma. There is a mass effect on the underlying brain, and the hematoma was large enough to warrant subsequent evacuation.

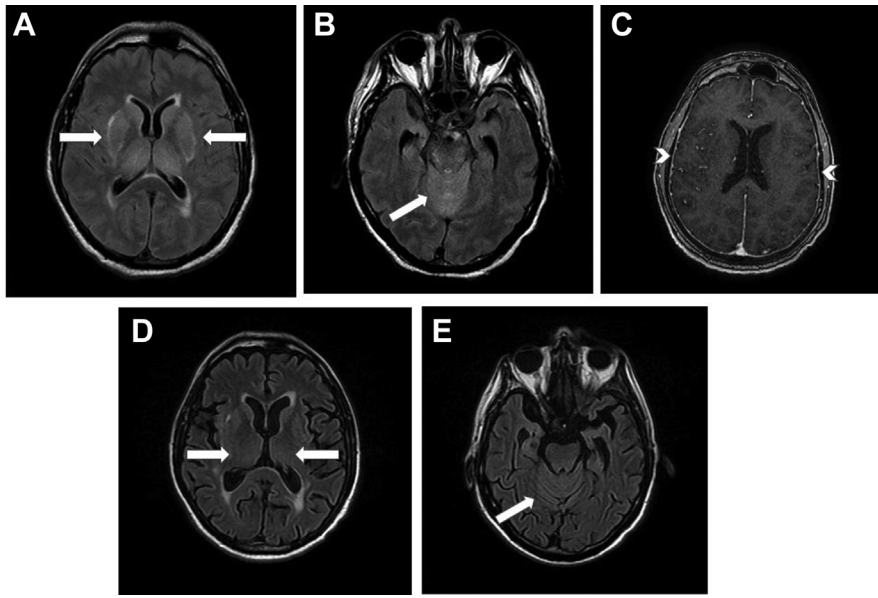

Fig. 13. Postoperative intracranial hypotension in an elderly man presenting with seizure and altered mental status after recent lumbar fusion that was complicated by durotomy. (*A*, *B*) Axial T2/FLAIR MR images of the brain show symmetric abnormal T2/FLAIR hyperintensity within the bilateral basal ganglia and thalami as well as within the superior cerebellum (*arrows*). (*C*) Axial postcontrast 3D T1-weighted MR image of the brain shows diffuse pachymeningeal enhancement (*arrowheads*) suggestive of intracranial hypotension. (*D*, *E*) Axial T2/FLAIR MR images of the brain 6 weeks later show resolution of the prior edema within the basal ganglia, thalami, and cerebellum (*arrows*).

become symptomatic and require evacuation to prevent herniation. Noncontrast head CT is the most appropriate examination to initially assess for postoperative hemorrhage, although MRI may detect smaller, more subtle hemorrhage. An extra-axial collection deep to a craniotomy often contains a combination of acute blood and fluid, so its density on CT may be lower than would be expected for purely acute hemorrhage. Extra-axial hematomas after craniotomy are usually extradural and located directly beneath the bone flap, but extradural hematomas may also occur adjacent to the bone flap margins or in a location remote from the flap.[33]

Parenchymal hemorrhage may also be expected postoperatively if the intervention was on the brain parenchyma or required traversal of the brain. For example, resection of an intra-axial tumor or placement of an external ventricular drain may result in a small amount of parenchymal hemorrhage surrounding the resection cavity or along the surgical tract. If the hemorrhage is larger than routinely observed, expands, or exerts significant mass effect, it may become clinically significant and warrant further intervention.

A unique type of parenchymal hemorrhage that may be observed after a craniotomy or even a spinal surgery is remote cerebellar hemorrhage. This occurs distant from the surgical site and is believed to reflect a form of hemorrhagic infarction that results from occlusion of posterior fossa bridging veins when the cerebellum sags in response to low CSF volume/intracranial hypotension.[34]

Intracranial hypotension induced by either an intracranial or spinal operative dural defect can cause low-pressure headaches and manifest on CT or MRI with findings

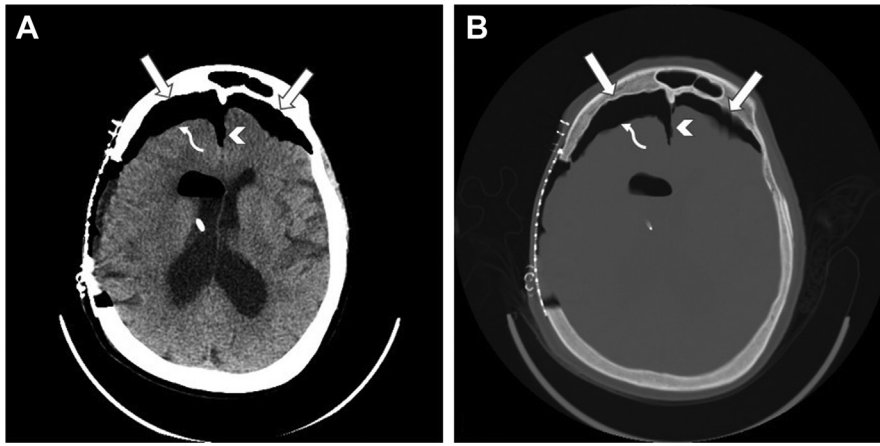

Fig. 14. Tension pneumocephalus in a patient who developed acute confusion 2 days following craniotomy. Axial noncontrast CT images of the head in brain (*A*) and bone (*B*) windows show bifrontal subdural gas (*straight arrows*) tracking into the interhemispheric fissure (*arrowheads*). The right frontal pneumocephalus exerts mass effect on the right frontal lobe (*curved arrows*).

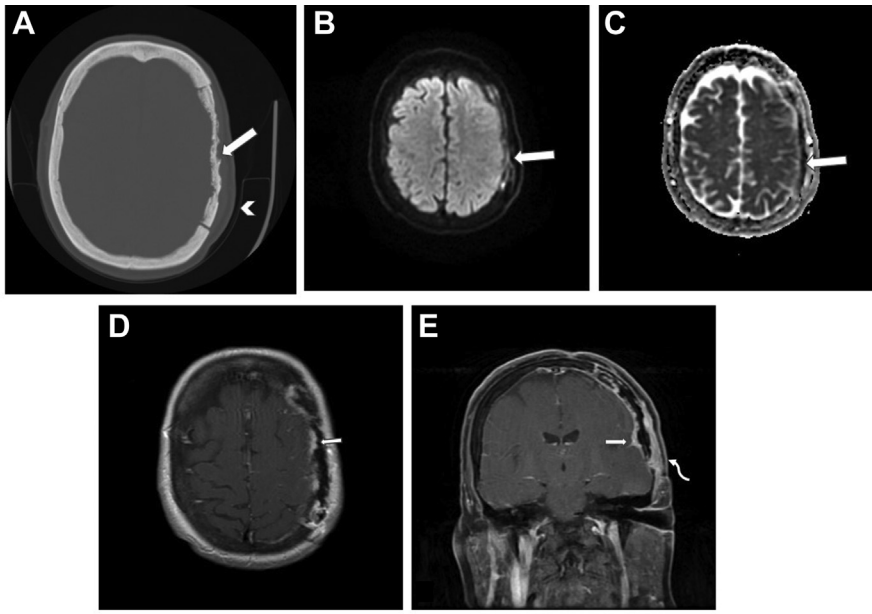

Fig. 15. Infected bone flap in patient with cellulitis of the overlying scalp 1 month after craniotomy. (*A*) Axial noncontrast CT image of the head in bone algorithm shows erosions and lytic changes (*straight arrow*) of the left frontoparietal bone flap with overlying soft tissue swelling (*arrowhead*). (*B*, *C*) Axial diffusion-weighted (*B*) and apparent diffusion coefficient (*C*) MR images of the head show restricted diffusion involving the bone flap (*straight arrows*). (*D*) Axial postcontrast T1-weighted MR image of the head shows abnormal dural enhancement deep to the craniotomy (*straight arrow*) that is thicker and more irregular than that normally observed after craniotomy. (*E*) Coronal postcontrast T1 fat-saturated MR image of the head shows abnormal dural (*straight arrow*) and soft tissue (*curved arrow*) enhancement concerning for phlegmon.

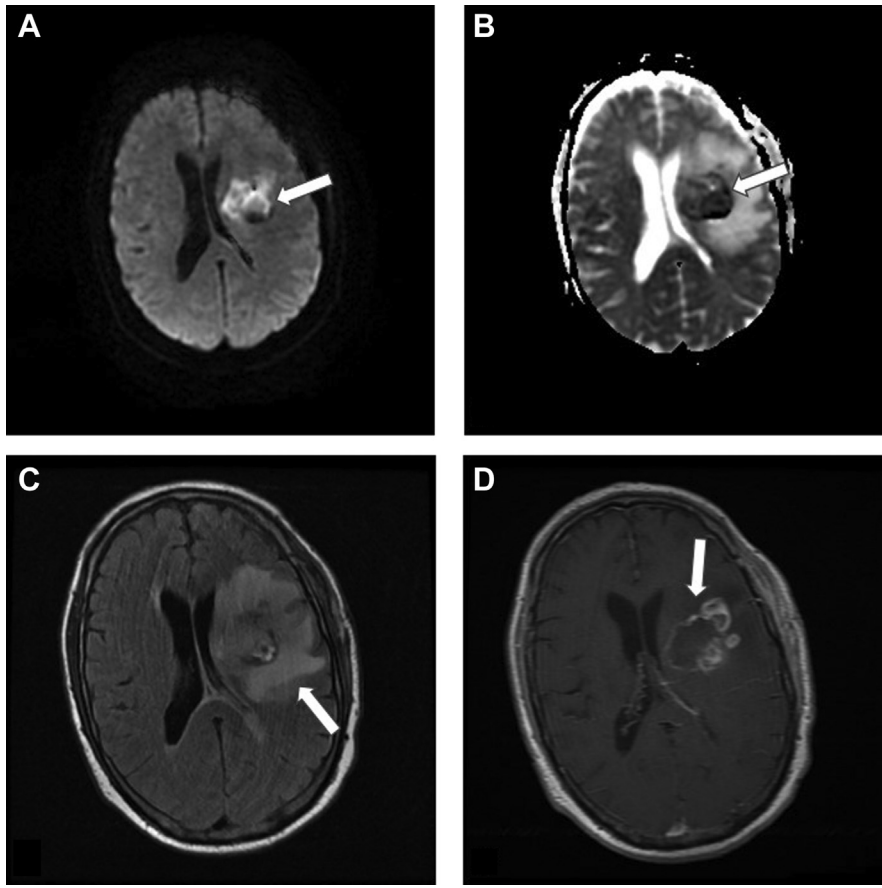

Fig. 16. Cerebral abscess following craniotomy. (*A, B*) Axial diffusion-weighted (*A*) and apparent diffusion coefficient (*B*) MR images of the brain show a collection in the left corona radiata deep to the craniotomy that demonstrates internal restricted diffusion (*arrows*). (*C*) Axial T2/FLAIR MR image of the brain shows confluent T2 hyperintensity surrounding the collection (*arrow*) compatible with vasogenic edema. (*D*) Axial postcontrast T1-weighted MR image of the brain shows peripheral enhancement of the collection (*arrow*). This constellation of imaging features most likely represents abscess.

of slumping brainstem, effacement of the suprasellar cistern, and decreased ventricular caliber as discussed in the section on fracture. However, additional findings of symmetric edema involving the bilateral basal ganglia, thalamus, and/or cerebellum or brainstem have been observed in the setting of postoperative intracranial hypotension[35] (**Fig. 13**).

Pneumocephalus is expected to a slight degree immediately following craniotomy, but when it exerts mass effect on the brain and is associated with neurologic decline, it is considered tension pneumocephalus and becomes a neurosurgical emergency. Imaging findings of this process include gas in the bifrontal subdural compartment, which impresses on and deforms the underlying brain parenchyma (**Fig. 14**). The subdural gas may also track into and widen the interhemispheric fissure.[36]

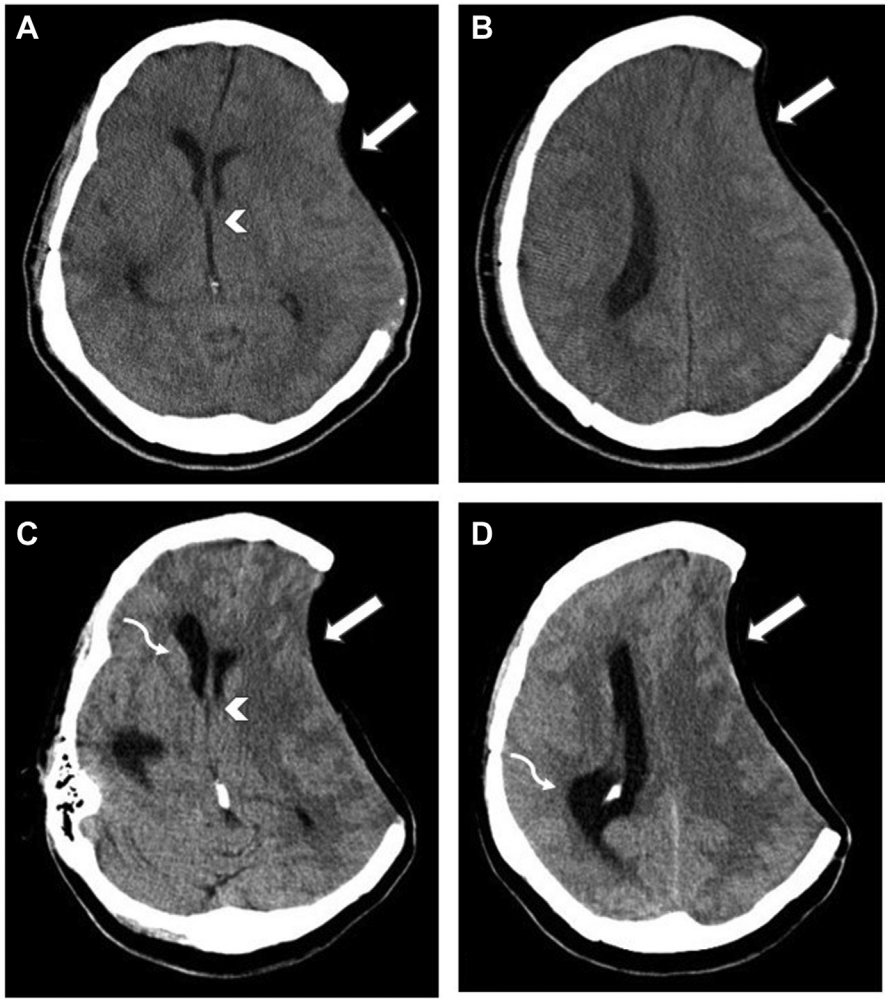

Fig. 17. Trephine syndrome in a patient 3 months after craniectomy and subsequent paradoxical herniation in the same patient following lumbar puncture. (*A*, *B*) Axial noncontrast CT images of the head demonstrate concave deformity of the left frontal lobe underlying the craniectomy defect (*arrows*). There is slight rightward midline shift at this time (*arrowhead*). (*C*, *D*) Axial noncontrast CT images of the head in the same patient after lumbar puncture reveal progressed concave deformity of the left frontal lobe (*arrow*) as well as progressed rightward subfalcine herniation (*arrowhead*) and interval dilation of the right lateral ventricle (*curved arrows*) indicating entrapment.

Infection

Postoperative infection may affect the craniotomy bone flap, extra-axial compartment, or brain. Bone flap infection usually manifests a few weeks after surgery and is often preceded by overlying cellulitis. Longer surgeries and repeat craniotomies are associated with a higher rate of bone flap infection, as are surgeries in which the paranasal sinuses are violated. CT and MRI can be useful in the detection of bone flap infection, although the CT findings of osteolysis may also be observed in old, devitalized bone flaps. MRI is therefore more reliable and demonstrates bone marrow edema and enhancement when a bone flap is infected (Fig. 15).

The most common extra-axial infection following craniotomy is extradural abscess. The subdural compartment is less frequently involved because postoperative infections often begin in the superficial soft tissues and spread first to the extradural region.[37] CT can be used to detect an extra-axial fluid collection, but MRI is more sensitive for determining whether it is infected. Both extradural abscesses and subdural empyemas demonstrate internal T2 hyperintensity as well as peripheral enhancement. Diffusion restriction of the contents of a rim-enhancing fluid collection generally indicates infection, but this sequence is less reliable in the postoperative setting, in part due to the presence of blood products that can also restrict diffusion.[38] In addition to these false-positive cases of extra-axial infection, false-negative rates of extradural abscess and subdural empyema are higher in postoperative patients: one study demonstrated a 47% false-negative rate for extradural abscess detection on diffusion-weighted imaging of postoperative patients.[38]

Brain or cerebral abscess may occur following craniotomy and demonstrates the same imaging features as extra-axial abscess but is located in the brain parenchyma (**Fig. 16**). In one large retrospective study, the number of patients with intracranial infection who developed a postoperative cerebral abscess was similar to the number of patients who developed a subdural empyema, about 15% of infected patients.[39]

Postcraniectomy

There are two postoperative phenomena unique to patients who have undergone craniectomy. Trephine syndrome or syndrome of the trephined manifests as headaches, seizures, dizziness, and excessive fatigue in the months following craniectomy. Imaging of these patients often reveals a sunken or concave morphology of the skin flap overlying the craniectomy (**Fig. 17**). The symptoms are thought to relate to altered CSF dynamics and reduced cerebral perfusion due to exposure of the intracranial contents to atmospheric pressure.[40] Cranioplasty leads to clinical improvement in some of these patients.

Paradoxical herniation is a rare complication of craniectomy and may be observed in patients with a large craniectomy defect who undergo subsequent CSF drainage via lumbar puncture or ventricular shunting. The decrease in CSF pressure in the setting of brain exposed to the external environment can result in atmospheric pressure overtaking intracranial pressure and causing herniation of the brain away from the craniectomy defect (see **Fig. 17**). Clinical manifestations of this process include depressed level of consciousness and focal neurologic deficits.[40] Paradoxical herniation should be emergently managed by increasing intracranial pressure via clamping of any ventricular catheters and perhaps performing cranioplasty.

SUMMARY

Headache can occur following trauma or surgery to the brain and may be associated with the specific pathologic processes described. In the acute setting following trauma or craniotomy, hemorrhage, edema, and vascular injury are among the causes of headache. Postcraniotomy infection has a more indolent course and delayed presentation. Recognizing the imaging features of these processes allows for prompt diagnosis and management.

CLINICS CARE POINTS

- Noncontrast CT of the brain is usually the best initial imaging tool to evaluate patients with headache following trauma or craniotomy.

- Brain MRI is more sensitive than CT for detecting certain posttraumatic and postoperative abnormalities such as DAI and infection.
- Extra-axial hematomas with mixed density on CT may contain hyperacute, hypodense blood products rather than simply acute on chronic hemorrhage.
- The diagnoses of postoperative tension pneumocephalus and paradoxical herniation should be based on both imaging features and clinical presentation.
- MRI is less reliable in demonstrating extra-axial infection in the postoperative setting than in nonoperative patients, with relatively high false-negative and false-positive rates.

DISCLOSURE

The author has nothing to disclose.

REFERENCES

1. Headache Classification Committee of the International Headache Society (HIS). The International Classification of Headache Disorders, 3rd edition. Cephalalgia 2018;38:1–211.
2. Lucas S, Hoffman JM, Bell KR, et al. A prospective study of prevalence and characterization of headache following mild traumatic brain injury. Cephalalgia 2014; 34:93–102.
3. Shih RY, Burns J, Ajam AA, et al. ACR Appropriateness Criteria Head Trauma. Available at: https://acsearch.acr.org/docs/69481/Narrative/. Am Coll Radiol. Accessed August 20, 2021.
4. Schweitzer AD, Niogi SN, Whitlow CT, et al. Traumatic brain injury: imaging patterns and complications. Radiographics 2019;39:1571–95.
5. Wei SC, Ulmer S, Lev MH, et al. Value of coronal reformations in the CT evaluation of acute head trauma. AJNR Am J Neuroradiol 2010;31:334–9.
6. Zacharia TT, Nguyen DT. Subtle pathology detection with multidetector row coronal and sagittal CT reformations in acute head trauma. Emerg Radiol 2010;17(2): 97–102.
7. Sieswerda-Hoogendoorn T, Postema FAM, Verbaan D, et al. Age determination of subdural hematomas with CT and MRI: a systematic review. Eur J Radiol 2014; 83(7):1257–68.
8. Iliescu IA. Current diagnosis and treatment of chronic subdural hematomas. J Med Life 2015;8(3):278–84.
9. Kolias AG, Chari A, Santarius T, et al. Chronic subdural haematoma: modern management and emerging therapies. Nat Rev Neurol 2014;10(10):570–8.
10. Tsutsumi K, Maeda K, Iijima A, et al. The relationship of preoperative magnetic resonance imaging findings and closed system drainage in the recurrence of chronic subdural hematoma. J Neurosurg 1997;87(6):870–5.
11. Zanini MA, de Lima Resende LA, de Souza Faleiros AT, et al. Traumatic subdural hygromas: proposed pathogenesis based classification. J Trauma 2008;64(3): 705–13.
12. Bodanapally UK, Dreizin D, Issa G, et al. Dual-energy CT in enhancing subdural effusions that masquerade as subdural hematomas: diagnosis with virtual high-monochromatic (190-keV) images. AJNR Am J Neuroradiol 2017;38(10):1946–52.
13. Al-Nashkabandi NA. The swirl sign. Radiology 2001;218(2):433.

14. Mata-Mbemba D, Mugikura S, Nakagawa A, et al. Traumatic midline subarachnoid hemorrhage on initial computed tomography as a marker of severe diffuse axonal injury. J Neurosurg 2018;129(5):1317–24.
15. Mata-Mbemba D, Mugikura S, Nakagawa A, et al. Intraventricular hemorrhage on initial computed tomography as marker of diffuse axonal injury after traumatic brain injury. J Neurotrauma 2015;32(5):359–65.
16. Perrein A, Petry L, Reis A, et al. Cerebral vasospasm after traumatic brain injury: an update. Minerva Anestesiol 2015;81(11):1219–28.
17. Alahmadi H, Vachhrajani S, Cusimano MD. The natural history of brain contusion: an analysis of radiological and clinical progression. J Neurosurg 2010;112(5):1139–45.
18. Yue JK, Winkler EA, Puffer RC, et al. Temporal lobe contusions on computed tomography are associated with impaired 6-month functional recovery after mild traumatic brain injury: a TRACK-TBI study. Neurol Res 2018;40(11):972–81.
19. Paterakis K, Karantanas AH, Komnos A, et al. Outcome of patients with diffuse axonal injury: the significance and prognostic value of MRI in the acute phase. J Trauma 2000;49(6):1071–5.
20. Linsenmaier U, Wirth S, Kanz KG, et al. Imaging minor head injury (MHI) in emergency radiology: MRI highlights additional intracranial findings after measurement of trauma biomarker S-100B in patients with normal CCT. Br J Radiol 2016;89:20150827.
21. Yuh EL, Mukherjee P, Lingsma HF, et al. Magnetic resonance imaging improves 3-month outcome prediction in mild traumatic brain injury. Ann Neurol 2013;73(2):224–35.
22. Baugnon KL, Hudgins PA. Skull base fractures and their complications. Neuroimaging Clin N Am 2014;24(3):439–65, vii-viii.
23. Hiremath SB, Gautam AA, Sasindran V, et al. Cerebrospinal fluid rhinorrhea and otorrhea: a multimodality imaging approach. Diagn Interv Imaging 2019;100(1):3–15.
24. Rischall MA, Boegel KH, Palmer CS, et al. MDCT venographic patterns of dural venous sinus compromise after acute skull fracture. AJR Am J Roentgenol 2016;207(4):852–8.
25. Kuo KH, Pan YJ, Lai YJ, et al. Dynamic MR imaging patterns of cerebral fat embolism: a systematic review with illustrative cases. AJNR Am J Neuroradiol 2014;35(6):1052–7.
26. Parizel PM, Demey HE, Veeckmans G, et al. Early diagnosis of cerebral fat embolism syndrome by diffusion-weighted MRI (starfield pattern). Stroke 2001;32(12):2942–4.
27. Kosova E, Bergmark B, Piazza G. Fat embolism syndrome. Circulation 2015;131(3):317–20.
28. Moen KG, Brezova V, Skandsen T, et al. Traumatic axonal injury: the prognostic value of lesion load in corpus callosum, brain stem, and thalamus in different magnetic resonance imaging sequences. J Neurotrauma 2014;31(17):1486–96.
29. Alhilali LM, Delic J, Fakhran S. Differences in callosal and forniceal diffusion between patients with and without postconcussive migraine. AJNR Am J Neuroradiol 2017;38:691–5.
30. Rutman AM, Vranic JE, Mossa-Basha M. Imaging and management of blunt cerebrovascular injury. Radiographics 2018;38(2):542–63.
31. Shim HS, Kang KJ, Choi HJ, et al. Delayed contralateral traumatic carotid cavernous fistula after craniomaxillofacial fractures. Arch Craniofac Surg 2019;20(1):44–7.

32. Rocha-Filho PA. Post-craniotomy headache: a clinical view with a focus on the persistent form. Headache 2015;55(5):733–8.
33. Sinclair AG, Scoffings DJ. Imaging of the post-operative cranium. Radiographics 2010;30:461–82.
34. Amini A, Osborn AG, McCall TD, et al. Remote cerebellar hemorrhage. AJNR Am J Neuroradiol 2006;27(2):387–90.
35. Hadizadeh DR, Kovacs A, Tschampa H, et al. Postsurgical intracranial hypotension: diagnostic and prognostic imaging findings. AJNR Am J Neuroradiol 2010; 31(1):100–5.
36. Michel SJ. The Mount Fuji sign. Radiology 2004;232(2):449–50.
37. Hlavin ML, Kaminski HJ, Fenstermaker RA, et al. Intracranial suppuration: a modern decade of postoperative subdural empyema and epidural abscess. Neurosurgery 1994;34(6):974–80.
38. Farrell CJ, Hoh BL, Pisculli ML, et al. Limitations of diffusion-weighted imaging in the diagnosis of postoperative infections. Neurosurgery 2008;62(3):577–83.
39. Dashti SR, Baharvahdat H, Spetzler RF, et al. Operative intracranial infection following craniotomy. Neurosurg Focus 2008;24(6):E10.
40. Akins PT, Guppy KH. Sinking skin flaps, paradoxical herniation, and external brain tamponade: a review of decompressive craniectomy management. Neurocrit Care 2008;9(2):269–76.